Quasi-classical trajectory-based non-equilibrium chemical reaction models for hypersonic air flows

Tapan K. Mankodi and R. S. Myong (명노신)[1)]

School of Mechanical and Aerospace Engineering and Research Center for Aircraft Core Technology, Gyeongsang National University, Jinju, Republic of Korea

Abstract:

Phenomenological models such as Park's widely used two temperature model over-predict the reaction rate coefficients at vibrationally cold conditions and under-predict it at vibrationally hot conditions. To this end, two new chemical reaction models, the non-equilibrium total temperature (NETT) and non-equilibrium piecewise interpolation (NEPI) models for the continuum framework are presented. The focus is on matching the reaction rate coefficients calculated using a quasi-classical trajectory (QCT) based dissociation cross-section database. The NETT model is an intuitive model based on physical understanding of the reaction at a molecular level. A new non-equilibrium parameter and the use of total temperature in the exponential term of the Arrhenius fit ensure the NETT model has a simple and straight-forward implementation. The efficacy of the new model was investigated for several equilibrium and non-equilibrium conditions in the form of heat bath simulations. Additionally, two-dimensional hypersonic flows around a flat blunt-body were simulated by employing various chemical reaction models, to validate the new models using experimental shock tube data. Park's two temperature model predicted higher dissociation rates, higher degree of dissociation leading to lower peak vibrational temperatures compared to those predicted by the new non-equilibrium

models. Overall, the present work demonstrates that the new non-equilibrium models perform better than Park's two temperature model, especially in simulations with a high degree of non-equilibrium, particularly as observed in re-entry flows.

Keywords: Non-equilibrium flow, chemical reaction modeling, hypersonic aerothermodynamics

[1)] Corresponding author: Tel: +82-55-772-1645. Email: myong@gnu.ac.kr.

I. Introduction

The field of non-equilibrium aerothermodynamics has experienced an increase in relevance and interest in recent times [1], not only for investigating flows around re-entry vehicles, but also in efforts to develop and design vehicles capable of sustained hypersonic flights, such as hypersonic glide vehicles. The kinetic energy in the flow goes through a rapid transformation to thermal energy across the shock wave on the fore-body of the vehicle. Phenomena such as vibrational energy excitation, chemical and ionization reactions, surface interactions such as recombination and ablation, and radiative heat transfer make the overall problem extremely complicated and challenging [2].

A wide range of computational methodologies has been developed to investigate the hypersonic gas flows, the most widely used method being computational fluid dynamic solvers based on the Navier-Stokes-Fourier (NSF) equations. The conservation laws for mass, momentum, and energy are solved over a domain discretized into a finite number of cells. The non-conserved quantities, namely stress tensor and heat flux, are modeled using Navier's law, based on Stokes' hypothesis, and Fourier's law, respectively, using temperature dependent transport coefficients. Vibrational energy excitation and chemical reactions are included in the system by adding respective equations for vibrational energy and species. The NSF solvers are based on the first-order constitutive laws and thus suffer from obvious short-comings when simulating flows with a high degree of thermal non-equilibrium.

In addition to these continuum-based computational strategies, the direct simulation Monte Carlo (DSMC) method developed by Bird [3–6] is a mesoscale particle method popular for investigating rarefied re-entry flows. Several phenomenological models for vibrational energy excitation [7] and chemical reactions [8–10] have been reported in the DSMC method.

In recent years, improved models have been developed for calculating inelastic and reaction cross-sections based on molecular dynamics calculations such as the quasi-classical trajectory (QCT) method [11]. These models have highlighted the remarkable difference in reaction rates predicted by the phenomenological and ab-initio based models. This discrepancy, in turn, results in differences in the flow properties and surface heat fluxes on the re-entry and glide vehicles.

The effect of vibrational excitation on dissociation and the effect of dissociation on vibrational energy distribution has been a subject of study for a long time [12, 13]. The relaxation times for these processes are often similar to flow times, resulting in a non-equilibrium nature. From the molecular point of view, there are insufficient collisions among molecules for the system to equilibrate. Compared with the vibrational energy, the rotational energy redistribution requires fewer collisions to equilibrate with the translational energy. Based on this observation, Park [2] in 1990 proposed a two temperature model to incorporate the non-equilibrium effects on chemical reactions. The temperature denoting the translational and rotational energies is known as the trans-rotational temperature (T_{tr}). The vibrational energy is represented by a separate temperature quantity known as the vibrational temperature (T_v). At higher temperatures and equilibrium conditions, a significant fraction of molecules populate the higher vibrational levels. The molecules in higher vibrational levels are more susceptible to dissociate than those placed in the lower vibrational levels. In the case of re-entry flows, due to insufficient collisions and longer vibrational relaxation times, the distribution of molecules is skewed towards the lower vibrational quantum states. This is the reason vibrational temperatures are lower than the trans-rotational temperature. Hence, it is reasonable to assume that the reaction rates for non-equilibrium flows ($T_v < T_{tr}$) would be lower than that in equilibrium flows.

Park suggested that the temperature supplied (T_a) to the Arrhenius reaction rate formula should be the geometric mean of the trans-rotational and vibrational temperatures:

$$T_a = \sqrt{T_{tr} T_v} \tag{1}$$

Various reports have suggested that, instead of using the geometric mean, the following relation for T_a is a better recommendation:

$$T_a = T_{tr}^{\alpha} T_v^{1-\alpha} \tag{2}$$

or in logarithmic expression,

$$\ln T_a = \alpha \ln T_{tr} + (1-\alpha) \ln T_v \tag{3}$$

with a parameter $\alpha = 0.7$ [1]. Note that this recovers Park's model when $\alpha = 0.5$. Also, the crucial role of the parameter α ($0 \leq \alpha \leq 1$) can be easily seen in the distributed importance of trans-rotational (T_{tr}) and vibrational temperatures (T_{vib}) in logarithmic scale.

Recently, improvements in computer architecture have encouraged the development of chemical reaction models [14–20] based on more theoretical foundations. These include the coarse-grains models [21–25] for dissociation and internal exchange based on ab-initio derived QCT rates. Molecular dynamics based methods such as the QCT method have been employed to calculate reaction cross-sections and reaction rate coefficients. These methods use highly accurate potential energy surfaces (PES), which are constructed using high fidelity ab-initio based computational chemistry algorithms. Luo *et al*. [26, 27] reported dissociation and exchange cross-sections for N2-O collisions and derived a non-equilibrium model for continuum solvers. Their analysis shows that Park's model, the coupled-vibration dissociation-vibration (CVDV) model [12], and the Macheret-Fridman model [13] were at least two orders inaccurate for the QCT based reaction rates in non-equilibrium conditions.

In addition to these, several authors have reported improved chemical reaction models [28, 29] for the continuum framework that can handle non-equilibrium dissociation rates efficiently. However, it is crucial to realize that, although Park's two-temperature model over-predicts dissociation rates at lower vibrational temperatures, it is widely used today because of its clear and simple implementation.

In the present work, the available collision-induced dissociation cross-sections [30–32] for nitrogen and oxygen systems were first used to obtain non-equilibrium reaction rate coefficients for a wide range for translational and vibrational temperatures. The data, as expected, largely deviates from the non-equilibrium reaction rate coefficients predicted by Park's two temperature model. Then, two chemical reaction models for non-equilibrium reaction rate coefficients suitable for the NSF equations are proposed.

The first model, the non-equilibrium total (or overall) temperature (NETT) model, is a more physically intuitive model based on a parameter defined on physical consideration, rather than pure empirical consideration and has a form similar to Park's two temperature model. The second model, non-equilibrium piecewise interpolation (NEPI), is a more computationally expensive model that predicts the non-equilibrium rates more accurately than the NETT model over a wide range of non-equilibrium conditions.

The performance of these models was then compared with the phenomenological Park's two temperature model for strong shock wave applications. The focus is presently limited to non-equilibrium reaction rates, and not the vibrational excitation rates, and the effects of dissociation in the post-reaction distribution of vibrational levels. This work will be investigated within the first-order NSF, and the second-order NCCR frameworks [33, 34] will be addressed at a later time.

Section II introduces the details of the cross-sections database. It also includes a comparison of equilibrium and non-equilibrium reaction rate coefficients calculated using the QCT cross-sections, Park's two-temperature model and the quantum kinetic (QK) reaction rates. Section III then describes the formulation of the two new models based on physical and numerical approaches. Validation of the two new models is discussed in Section IV. Results for the comparative study using the two new models and Park's model for heat bath simulations and hypersonic flow over a flat blunt-body are also described.

II. QCT Cross-Sections and Reaction Rate Coefficients

Dissociation reactions can be divided into two classes: 1) the dissociation of molecules after colliding with an atom and 2) the dissociation of molecules upon colliding with another molecule. The dissociation of nitrogen after colliding with atomic or molecular nitrogen requires N_3 and N_4 PESs, respectively. Similarly, oxygen dissociation requires O_3 and O_4 PESs. Highly accurate PESs employing complete active space self-consistent field (CASSCF) and second-order perturbation theory (CASPT2) ab-initio computational chemistry methods for N_3 [30], O_3 [30], N_4 [35] and O_4 [36] systems have been reported in recent years. Their analytical least square fits are available on PotLIB [37]. Using these PESs, ensemble averaged databases of the reactive cross-sections (σ) of the dissociations $N_2 + N \rightarrow 3N$ [30], $O_2 + O \rightarrow 3O$ [30], $N_2 + N_2 \rightarrow N_2 + 2N$ [31] and $O_2 + O_2 \rightarrow O_2 + 2O$ [32] as a function of relative translational velocity, rotational and vibrational levels have been reported and tabulated in the supplementary materials of the respective source papers.

In the present work, these cross-section databases have been utilized to obtain the reaction rate coefficients. Reaction rate coefficients are calculated by integrating the dissociation cross-sections over the Maxwell-Boltzmann distribution functions for translational, rotational, and

vibrational energies using the given respective translational (T), rotational (T_R), and vibrational (T_V) temperatures. The equilibrium reaction rate coefficients can be obtained by employing equal temperatures for the three modes.

The general formula for obtaining reaction rate coefficients for atom-molecule system as a function of various temperatures is:

$$k(T,T_R,T_V) = \frac{1}{Q_V}\sum_v \exp\left(-\frac{E_{v,0}}{k_b T_V}\right)\frac{1}{Q_J}\sum_j g_j(2j+1)\exp\left(-\frac{E_{v,j}}{k_b T_R}\right) \times N_A\left(\frac{2}{\pi}\right)^{1/2}\left(\frac{\mu}{k_B T}\right)^{3/2}\int_0^\infty \sigma(v,j,V)\exp\left(-\frac{\mu V^2}{2k_B T}\right)V^3 dV \quad (4)$$

where Q_V and Q_R are the partition functions for the vibrational and rotational modes of energy, $E_{v,j}$ is the ro-vibrational energy for the level (j, v) using spectroscopy constants, g_j is the nuclear degeneracy for rotational levels, V is the relative velocity, μ is the reduced mass, and N_A and k are Avogadro's number and the Boltzmann constant, respectively. For molecule-molecule collisions, the reaction rate coefficients are calculated using a similar formula with additional summation over ro-vibrational levels of the second molecule, and the cross-section is a function of the ro-vibrational levels of both the molecules in addition to their relative speed.

Experimental data for the reaction rate coefficients using shock tube techniques have been reported [38-42] for different ranges of temperatures at equilibrium conditions. Employing these databases, first Baulch [43] and later Park recommended Arrhenius fit parameters for important reactions pertaining to air chemistry. The parameters recommended by Park and his two-temperature model are widely used data for air chemistry. Recently, Scanlon *et al*. [44] reported a different set of Arrhenius parameters for chemical reactions in the air using the quantum kinetic chemical reaction model by Bird [9]. The reaction rate coefficients obtained using the

dissociation cross-sections have been validated against experimental shock tube data reported elsewhere.

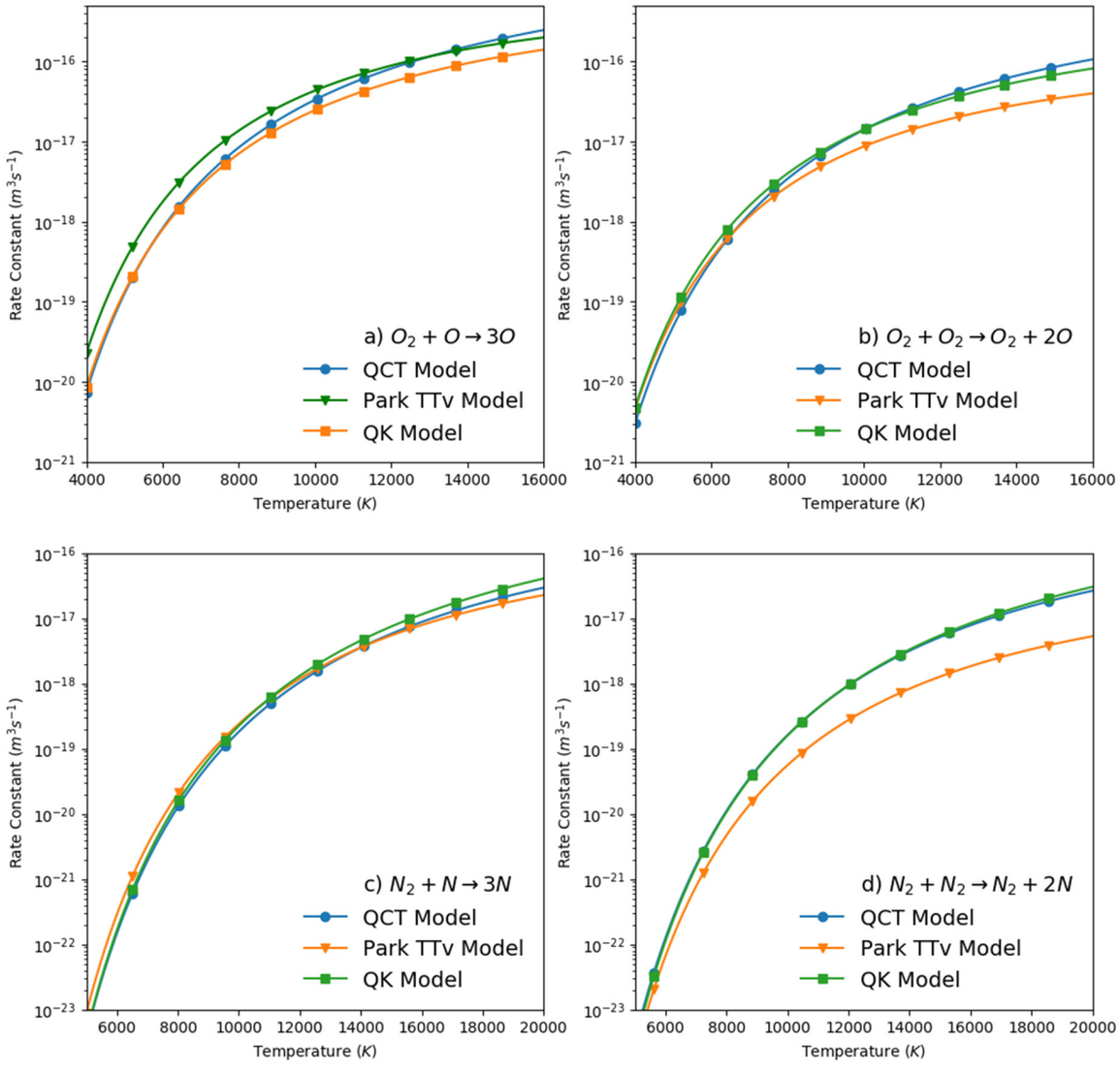

Fig. 1. Variation of reaction rate coefficients with temperature at equilibrium conditions obtained using the QCT calculated dissociation cross-section, Park's two temperature model and QK fit for systems a) $O_2 + O \rightarrow 3O$, b) $O_2 + O_2 \rightarrow O_2 + 2O$, c) $N_2 + N \rightarrow 3N$ and d) $N_2 + N_2 \rightarrow N_2 + 2N$.

Comparisons of the reaction rate coefficients of dissociation using the cross-section data against various Arrhenius fits employing Park and QK derived parameters are shown in Fig. 1. Figure 1 (a)-(d) shows a comparison of the reaction rates constants for systems involving the dissociation of 1) oxygen with atomic oxygen, 2) oxygen with molecular oxygen, 3) nitrogen with atomic nitrogen and 4) nitrogen with molecular nitrogen, respectively. It is clear from Fig. 1 that, at equilibrium conditions, the reaction rate coefficients calculated using the collision induced dissociation cross-sections are in reasonable agreement with the Arrhenius fits suggested by Park and Scanlon *et al*. The only noticeable disagreement is the difference between the reaction rate coefficients for the dissociation $N_2 + N_2 \rightarrow N_2 + 2N$ (shown in Fig. 1 (d)) for the QCT data with the Arrhenius fit suggested by Park. However, the QCT reaction rate coefficients are an excellent match with the Arrhenius data suggested by Scanlon *et al*. Further, the QK data and Arrhenius fit suggested by Scanlon *et al*. are in good agreement with the DSMC results of Gallis *et al*. [45]. The best fitted parameters in Arrhenius form for the present set of equilibrium reaction rate coefficients are reported in Table I.

Table I Parameters for fitting the Arrhenius equation ($k = AT^{\eta}\exp(-D/T)$) (m^3s^{-1}).

Reaction	A(m^3s^{-1})	η	D(K)
$O_2 + O \rightarrow 3O$	2.0315×10^{-13}	-0.3185	57932.32
$O_2 + O_2 \rightarrow O_2 + 2O$	2.25124×10^{-14}	-0.1855	57041.18
$N_2 + N \rightarrow 3N$	8.5145×10^{-12}	-0.7116	111100.05
$N_2 + N_2 \rightarrow N_2 + 2N$	1.8048×10^{-12}	-0.5703	109921.97

Tables II and III show a comparison of non-equilibrium reaction rate coefficients for the oxygen and nitrogen system, respectively, for various combinations of trans-rotational and vibrational temperatures as calculated using the QCT cross-section data with those reported by Chaudhry *et al.* [18] and Bender *et al*. [15]. It is evident from the tabulated values that the non-equilibrium reaction rate coefficients employing the QCT data agree well with data reported elsewhere.

Table II Comparison of non-equilibrium reaction rate coefficients calculated in the present work with reported values for oxygen system (Chaudhry *et al.* [18]) T_{tr}=10000 K

Tv	$O_2 + O \rightarrow 3O$		$O_2 + O_2 \rightarrow O_2 + 2O$	
	Mankodi *et al*.[30]	Chaudhry *et al*.[18]	Mankodi *et al*.[32]	Chaudhry *et al*.[18]
5000 K	3.429×10^{-18}	1.140×10^{-18}	4.327×10^{-18}	1.046×10^{-18}
10000 K	3.103×10^{-17}	8.695×10^{-17}	1.390×10^{-17}	1.215×10^{-17}

Table III Comparison of non-equilibrium reaction rate coefficients calculated in the present work with reported values for nitrogen system (Bender *et al.* [15]) T_{tr}=20000 K

Tv	$N_2 + N \rightarrow 3N$		$N_2 + N_2 \rightarrow N_2 + 2N$	
	Mankodi *et al*.[30]	Bender *et al*.[15]	Mankodi *et al*.[31]	Bender *et al*.[15]
10000 K	7.803×10^{-18}	2.903×10^{-18}	9.029×10^{-18}	2.043×10^{-18}
20000 K	2.952×10^{-17}	1.722×10^{-17}	2.647×10^{-17}	1.663×10^{-17}

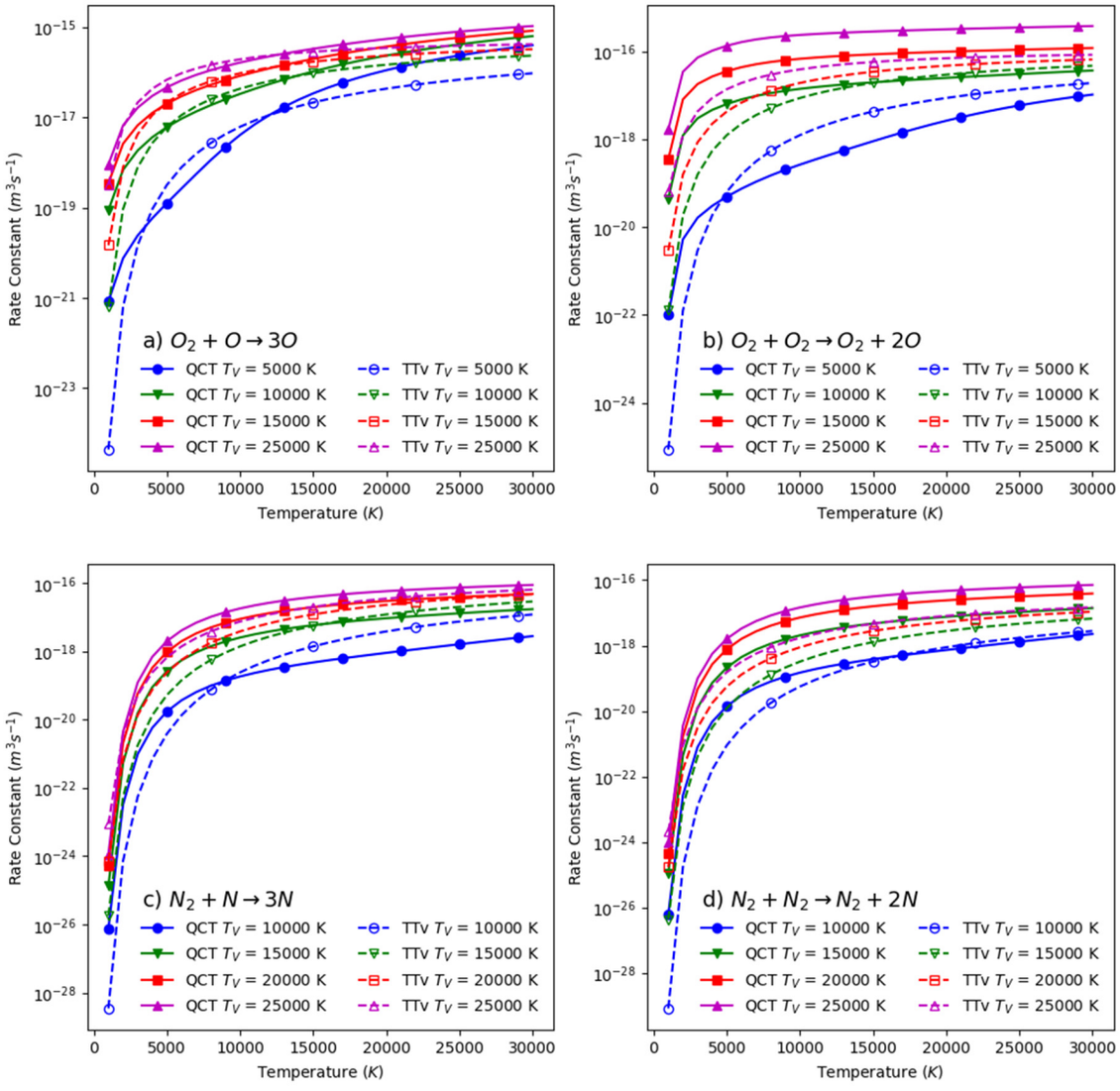

Fig. 2. Variation of reaction rate coefficients with trans-rotational temperature (T) at non-equilibrium conditions for different vibrational temperatures (Tv) obtained using the QCT calculated dissociation cross-section and Park's two temperature model for systems a) O_2 +O → 3O, b) O_2 + O_2 → O_2 + 2O, c) N_2 + N → 3N and d) N_2 + N_2 → N_2 + 2N.

A comparison of non-equilibrium reaction rate coefficients with trans-rotational temperatures for various vibrational temperatures between Park's two temperature model and those calculated using the QCT cross-section database is shown in Fig. 2. Park's original formulation with α =0.5,

used for calculating the non-equilibrium reaction rate coefficients, is represented by the broken lines in Fig. 2. Again, Fig. 2 (a)-(d) shows the non-equilibrium reaction rate coefficients for the dissociation of oxygen with atomic oxygen, 2) oxygen with molecular oxygen, 3) nitrogen with atomic nitrogen and 4) nitrogen with molecular nitrogen, respectively.

In contrast to the equilibrium reaction rates, the differences between the reaction rates calculated using the QCT cross-sections and Park's two temperature model are significant. In general, it can be inferred that at lower trans-rotational temperatures ($T < T_V$), the two-temperature model under-predicts dissociation rates while at higher trans-rotational temperatures ($T > T_V$), the two-temperature model over-predicts the dissociation rates. This effect is particularly amplified at lower vibrational temperatures, as shown in Fig. 2, at $T_V = 5000$ K and $T_V = 10000$ K.

At higher vibrational temperatures, the two-temperature model with Park's fitting parameter under-predicts the dissociation rate for the entire trans-rotational temperature range. In the case of molecule-molecule collisions, as shown in Fig. 2 (b) and (d), the difference between the dissociation rates for the highest vibrational temperature ($T_V = 25000$K) is close to two orders of magnitude. This large deviation is obvious given that there is a significant difference in the equilibrium rates at higher temperatures as shown in Fig. 1.

It must be noted that a similar disagreement is observed between the QCT based non-equilibrium reaction rates and those of the two temperature model employing the Arrhenius fitting parameters suggested by Scanlon *et al*., as noted in the comparison with the two temperature model employing Park's fitting parameters.

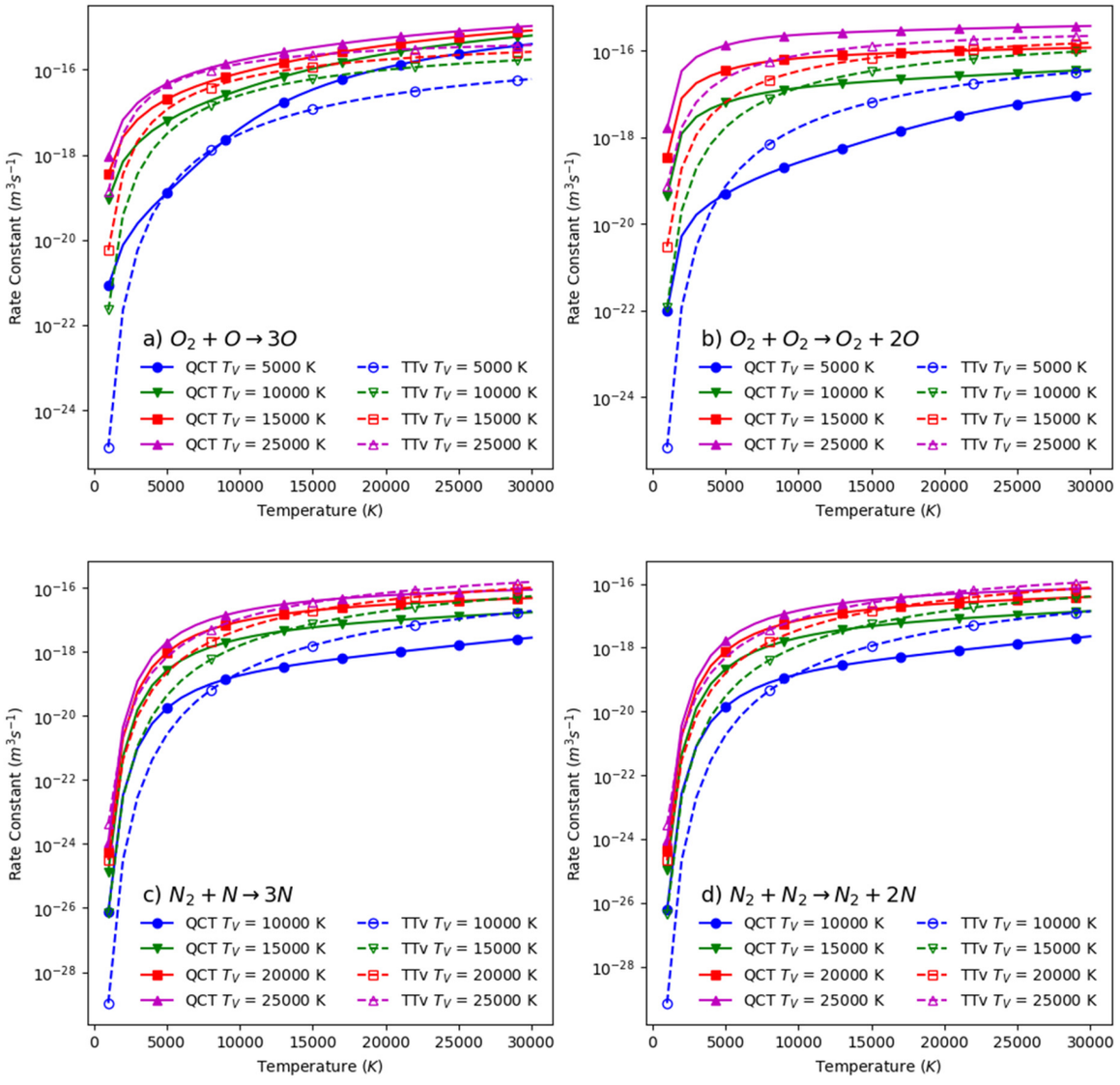

Fig. 3. Variation of reaction rate coefficients with trans-rotational temperature (T) at non-equilibrium conditions for different vibrational temperatures (T_V) obtained using the QCT calculated dissociation cross-section and Park's two temperature model and new Arrhenius parameters for systems a) O_2+O → 3O, b) O_2+O_2 → O_2 +2O, c) N_2+N → 3N and d) N_2 +N_2 → N_2+2N.

Further, a comparison of non-equilibrium rates using the two temperature model employing the new parameters tabulated in Table I is also shown in Fig. 3. A clearer trend emerges from this figure compared with Fig. 2. The difference is inherently due to the non-equilibrium conditions and is not dependent on the choice of the fitting parameters. It is also clear from comparative studies that the effect of non-equilibrium on reaction rates and consequently on the degree of dissociation should be handled in an appropriate manner when simulating flows with a high degree of non-equilibrium, such as re-entry flows.

III. Non-Equilibrium Dissociation Models

In the case of equilibrium conditions, the natural logarithm of the reaction rate coefficients generally has a downward sloping linear relation with the inverse of temperature. A pre-exponential term T^{η} is added to the relation to provide a more accurate representation. However, in non-equilibrium conditions, the behavior of the logarithm of the reaction rate coefficient with the inverse of the trans-rotational temperature at various vibrational temperatures is highly non-linear. The degree of non-linearity is more striking at lower vibrational temperatures, where the difference in the reaction rate coefficient predicted by Park's two temperature model and those calculated using the QCT cross-section data is enormous, often more than a few orders of magnitude.

In the present work, two new models are proposed to fit the non-equilibrium reaction rate coefficients. The first fitting model, the non-equilibrium total temperature (NETT) model, is developed with a sounder physical basis, and at the same time is easier to implement with lower computational overheads. As stated in the previous section, it is obvious that the deviations between the QCT calculated non-equilibrium reaction rate coefficients and those predicted by the phenomenological two temperature model with Park's Arrhenius parameters are bound to be

significant. It is evident from Fig. 3 that the two temperature model with new Arrhenius fitting parameters again over-predicts reaction rates in vibrationally cold conditions and under-predicts at vibrationally hot conditions. The new models are designed to overcome this issue. The NETT model includes an additional term in the Arrhenius equation that requires a new temperature-based non-dimensional non-equilibrium parameter.

The non-equilibrium parameter introduced takes the following form:

$$\beta = \frac{T_v}{T_{tr}} \tag{5}$$

where T_v and T_{tr} are the vibrational and trans-rotational temperatures, respectively. The range of the non-dimensional parameter β is between 0 and ∞. Vibrationally cold conditions would imply that vibrational temperatures are lower than the trans-rotational temperature, or β is less than 1. In contrast, when β > 1, the conditions would be vibrationally hot. At equilibrium, the value of non-equilibrium parameter would be 1. The following changes are made in the Arrhenius equation to handle non-equilibrium conditions in a sounder manner:

- The pre-exponential factor is assumed to be β^{χ} where β is the non-equilibrium parameter and χ is a new constant. The parameter χ is a positive quantity.
- The total (or overall) temperature is employed in the formulation as the controlling temperature, instead of Park's two temperature term ($\sqrt{TT_v}$) or the trans-rotational temperature. The total temperature is calculated using,

$$T_t = \frac{\delta_{tr} T_{tr} + \delta_{vib} T_v}{\delta_{tr} + \delta_{vib}}, \tag{6}$$

where δ_{tr} (δ_{tr} = 3+ 2 = 5) and δ_{vib} ($0 < \delta_{vib} < 2$) are the degree of freedom for the trans-rotational energy and vibrational energy, respectively. The equation can be rewritten in the following instructive form,

$$T_t = \alpha T_{tr} + (1-\alpha) T_v , \tag{7}$$

where

$$\alpha = \frac{\delta_{tr}}{\delta_{tr} + \delta_{vib}} . \tag{8}$$

Note that α has a physical meaning instead of being just an adjustable parameter in Eqn. (2). The trans-rotational degrees of freedom per molecule is the summation of three translational degrees of freedom and two rotational degrees of freedom. The vibrational degrees of freedom are defined as,

$$\delta_{vib} = \frac{2e_{vib}}{R_S T_V} , \tag{9}$$

where R_S is the specific gas constant and e_{vib} is the vibrational energy per molecule defined as,

$$e_{vib} = \frac{R_S \theta_{vib}}{\exp(\theta_{vib} / T_V) - 1} , \tag{10}$$

where θ_{vib} is the characteristic temperature for vibrational excitation.

Finally, the new NETT model assumes the following form,

$$k(T_{tr}, T_v) = A \beta^{\chi} T_t^{\eta} \exp\left(-\frac{D}{T_t} \right) , \tag{11}$$

where A, χ, η and D are parameters. The values of the parameters are tabulated in Table IV.

At collisional level, the total energy of the interacting entities is the factor that affects the outcome of an interaction. The total temperature, measuring the degree of the total energy in an interaction, is hence a more intuitive and a better choice for the controlling temperature rather than the trans-rotational temperature or the Park's two temperature term. The non-equilibrium term in the new formulations provides the additional liberty to fit the data in a better way. However, the degree of non-linearity in the non-equilibrium reaction rates is immense and thus the parameters for the present NETT model fit are weighted more for data at equilibrium conditions and vibrationally cold conditions, where the trans-rotational temperature is greater than the vibrational temperature. Despite this limitation, the model works well for all practical applications such as flow conditions encountered by a re-entry object.

Table IV. NETT model parameters.

Reaction	A($m^3 s^{-1}$)	χ	η	D(K)
$O_2 + O \rightarrow 3O$	2.0871×10^{-16}	-0.382	0.526	57923.32
$O_2 + O_2 \rightarrow O_2 + 2O$	4.967×10^{-19}	-0.906	2.387	57041.18
$N_2 + N \rightarrow 3N$	1.487×10^{-20}	-1.342	3.948	111100.05
$N_2 + N_2 \rightarrow N_2 + 2N$	4.921×10^{-21}	-1.426	3.944	109921.97

The second new model, the non-equilibrium piecewise interpolation (NEPI) model, is based on a piece-wise numerical fit. A different set of fitting parameters are obtained at different vibrational temperatures ranging from 1000 K to 30000 K with an interval equal to 1000 K. The analytical function used for fitting is a function of the trans-rotational temperature and is modeled to take the following form:

$$k_{T_V}(T_{tr}) = AT_{tr}^{\eta} \exp\left(-\frac{D}{T_{tr}^{m}}\right) \tag{12}$$

where A, η, D and m are parameters. The values of these parameters for the thirty different vibrational temperatures for various dissociation reactions are tabulated in the Supplementary Materials. The parameters to be employed for vibrational temperatures other than the tabulated temperatures are obtained by linear interpolation in order to obtain a non-equilibrium reaction rate coefficient for any given combination of temperatures.

Table V shows the quality of the fitting of the two non-equilibrium chemical reactions models against the data calculated using the QCT cross-section database. In addition to the new models, the error analysis also includes the deviation in non-equilibrium rates predicted by the two temperature model employing Park's Arrhenius fitting parameters and the new fitting parameters reported in the present work. L1 or mean error is calculated using

$$L1 = \frac{\sum_{i=1}^{N} |\ln(k_{i,QCT}) - \ln(k_{i,fit})|}{N}, \tag{13}$$

where k_{QCT} and k_{fit} are non-equilibrium reaction rates calculated using the QCT cross-section and the fitting method, respectively. Similarly, the L2 or the root mean square error, is calculated using

$$L2 = \sqrt{\frac{\sum_{i=1}^{N} (\ln(k_{i,QCT}) - \ln(k_{i,fit}))^2}{N}}. \tag{14}$$

It is clear that the two temperature model employing either Park's suggested Arrhenius fitting parameters or the new set of parameters reported in the present work are highly inaccurate. In comparison, the two new models proposed in the present study work fairly well and match the

non-equilibrium case better than the traditional phenomenological models. The NEPI model is obviously a better model and fits the non-equilibrium reaction rate coefficients data excellently when compared to the NETT model. Because the parameters of the NETT model are calculated using weighted least square fits, which allow better fitting in vibrationally cold conditions, it is highly inaccurate at extreme temperatures in vibrationally hot conditions, and hence the L1 and L2 errors are significantly larger than those for the present NEPI model fit.

Table V. Error analysis.

Method	L1	L2
$O_2 + O \rightarrow 3O$		
Two temperature (Park's Arrhenius coeff.)	0.911	1.6924
Two temperature (new Arrhenius coeff.)	0.9341	2.001
New NETT model	0.1573	0.2480
New NEPI model fit	0.0714	0.1941
$O_2 + O_2 \rightarrow O_2 + 2O$		
Two temperature (Park's Arrhenius coeff.)	1.5061	1.8503
Two temperature (new Arrhenius coeff.)	1.1465	1.7023
New NETT model	0.3026	0.4827
New NEPI model fit	0.0411	0.0900
$N_2 + N \rightarrow 3N$		
Two temperature (Park's Arrhenius coeff.)	1.4802	2.4889
Two temperature (new Arrhenius coeff.)	1.5034	2.6175
New NETT model	0.5545	0.8267
New NEPI model fit	0.1370	0.2238
$N_2 + N_2 \rightarrow N_2 + 2N$		
Two temperature (Park's Arrhenius coeff.)	2.0631	2.9329

Two temperature (new Arrhenius coeff.)	1.4984	2.5920
New NETT model	0.5546	0.8255
New NEPI model fit	0.1360	0.2237

IV. Simulations and Results

The governing equations for modeling hypersonic flows in the present work are the Navier-Stokes-Fourier (NSF) equations with additional equations for the vibrational energy exchange and chemical reactions. The state-of-the-art open-source hypersonic solver, hy2Foam, based on the OpenFOAM rhoCentralFoam solver, was used in the present simulations. The hypersonic solver can handle non-equilibrium NSF equations, finite rate chemistry, and chemistry-vibration coupling. The hy2Foam solver includes several chemistry databases, transport models, mixing rule models, turbulence models, and relevant boundary conditions such as the Maxwell velocity slip and Smoluchowski temperature jump conditions. The new chemical reaction models, NETT and NEPI models, were added to the existing list of chemical reaction models as additional functions.

The conservation laws for mass, momentum, and energy are:

$$\frac{\partial \rho}{\partial t} + \nabla \cdot (\rho \mathbf{u}) = 0 , \tag{15}$$

$$\frac{\partial \rho \mathbf{u}}{\partial t} + \nabla \cdot (\rho \mathbf{u}\mathbf{u}) + \nabla \cdot (p\mathbf{I} + \boldsymbol{\Pi}) = 0 , \tag{16}$$

$$\frac{\partial \rho E}{\partial t} + \nabla \cdot ((\rho E + p)\mathbf{u}) + \nabla \cdot (\boldsymbol{\Pi} \cdot \mathbf{u} + \mathbf{Q} + \mathbf{Q}_{\mathrm{V}}) = 0 , \tag{17}$$

where $\boldsymbol{\Pi}$, $\mathbf{Q}$, and $\mathbf{Q}_{\mathrm{V}}$ are non-conserved variables; viscous stress, heat flux, and heat flux for the vibrational energy mode. The viscous stress and heat flux are calculated using Navier's law with

the Stokes' hypothesis and Fourier's law, respectively. In addition to these equations, the species conservation equation (ρ_s where s is the index of species) and vibrational energy equation (E_v) are included:

$$\frac{\partial \rho_s}{\partial t} + \nabla \cdot (\rho_s \mathbf{u}) + \nabla \cdot (\rho_s \mathbf{v_s}) = w_s \,, \tag{18}$$

$$\frac{\partial \rho E_v}{\partial t} + \nabla \cdot (\rho E_v \mathbf{u}) + \nabla \cdot \mathbf{Q_v} = w_v \,. \tag{19}$$

These equations, unlike the conservation laws (15)-(17), have a non-zero source term due to chemical reactions, and the non-equilibrium between the trans-rotational and vibrational energy modes, respectively.

The simulations considered in this work are categorized into two bins: heat bath simulations and shock tube studies. The first category of simulations, the heat bath simulations, is used to investigate the effect of reactions on the relaxation of energy modes in hypothetical non-equilibrium initial conditions. The second batch of simulations is intended to validate the shock tube results produced by Ibraguimova *et al*. [46].

A. Heat Bath Simulations

A heat bath is a zero-dimensional case study consisting of a unit sized single cell as its domain, initialized at hypothetical conditions and made to relax towards the final equilibrium conditions. The effect of various chemical reaction models on the evolution of various properties, such as the temperatures pertaining to different modes of energy, and the mole-fractions of various species, are analyzed.

The heat bath simulations were grouped into two systems, an oxygen system and a nitrogen system. For the oxygen systems, the initial mole fractions of the atomic dissociated oxygen and

molecular undissociated oxygen were 0.5 each. Similarly, the nitrogen systems initially consist of equal mole-fractions of atomic and molecular nitrogen. Generally, the backward reaction rate coefficients for the recombination reactions are calculated using the equilibrium constant and forward reaction rate coefficients. The simulations here are focused on the effect of non-equilibrium on dissociation, and hence reverse recombination re-actions are ignored in the simulations. For each system, an additional three classes of simulations were conducted for various temperature conditions.

The first class of simulation was performed at equilibrium conditions with initial trans-rotational and vibrational temperatures equal to 15000 K. The second class of simulations investigated vibrationally cold conditions, where the vibrational temperature is lower than the trans-rotational temperature. The initial trans-rotational and vibrational temperatures were set at 25000 K and 10000 K, respectively. The final class of simulations has the opposite set of initial trans-rotational and vibrational temperatures, and denotes vibrationally hot conditions.

For each class of simulations, simulations were run for the three chemical reaction models: the traditional Park's two temperature $\sqrt{TT_V}$ model, the new NETT model, and the new NEPI model. The Arrhenius parameters used in Park's two temperature model are the original values recommended by Park. That is, the value of α in equation (2) is set to 0.5 to reproduce the original and the most widely used form of Park's two temperature model. The initial pressure is set to the standard pressure for all simulations. The time-step for the simulations is set at 1×10^{-10}s and the evolution of systems is tracked till the final time becomes equal to 1×10^{-2}s.

In addition to the NSF based simulations, 0D DSMC simulations with and ab-initio based chemical reaction model [23, 27], and the variable sphere hard (VHS) model with parameters calculated at high temperature (1000 K) reference, for modeling total collision cross-sections,

and temperature dependent Larsen-Borgnakke (LB) [12] for vibrational relaxation, were performed. The same cross-section databases used to calculate the non-equilibrium reaction rate coefficients that served as the basis for the present non-equilibrium models were employed in the DSMC simulations. The rotational relaxation parameter was set to 1.0 so that the translational and rotational energies equilibrate with each other and simulate the similar two temperature condition employed in the NSF simulations. Experimental reproductions for heat bath simulations at the specified initial conditions do not exist and hence DSMC simulations were performed.

It is important to note that the DSMC simulations are employed as an additional tool to improve confidence in the new non-equilibrium chemical reaction models over the traditional phenomenological models, rather than as a straightforward validation of the new models.

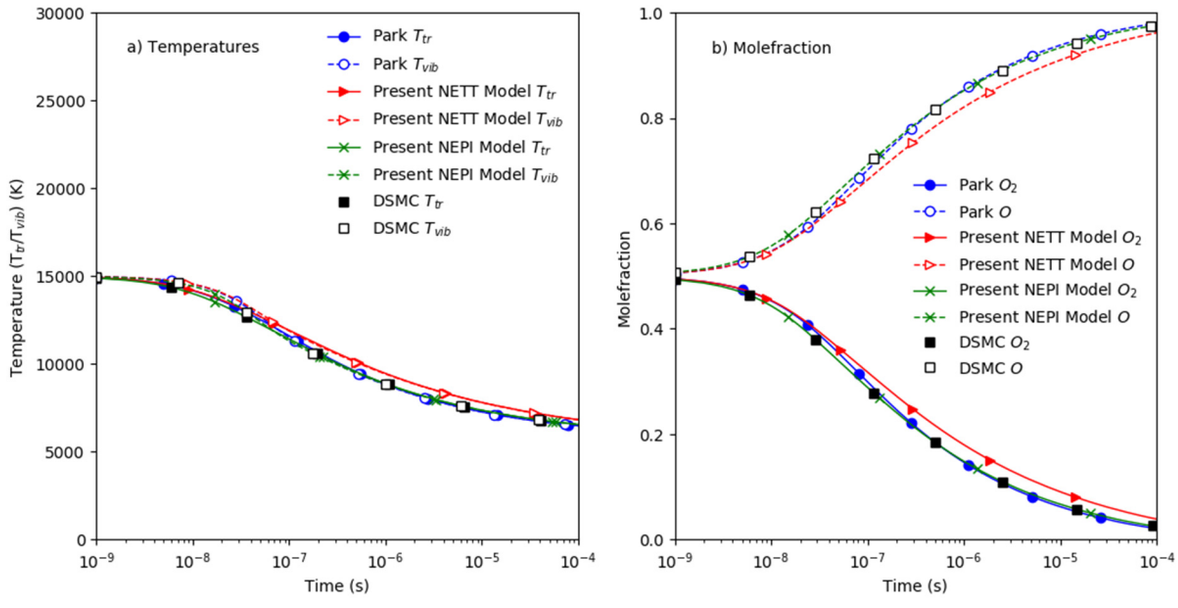

Fig. 4. Comparison of evolution of a) trans-rotational and vibrational temperatures b) mole-fraction of O and O_2 for simulation starting with equilibrium conditions, $T_{tr} = T_{vib}$ =15000 K and

employing Park's two temperature model, NETT model and NEPI model in NSF framework and DSMC simulation.

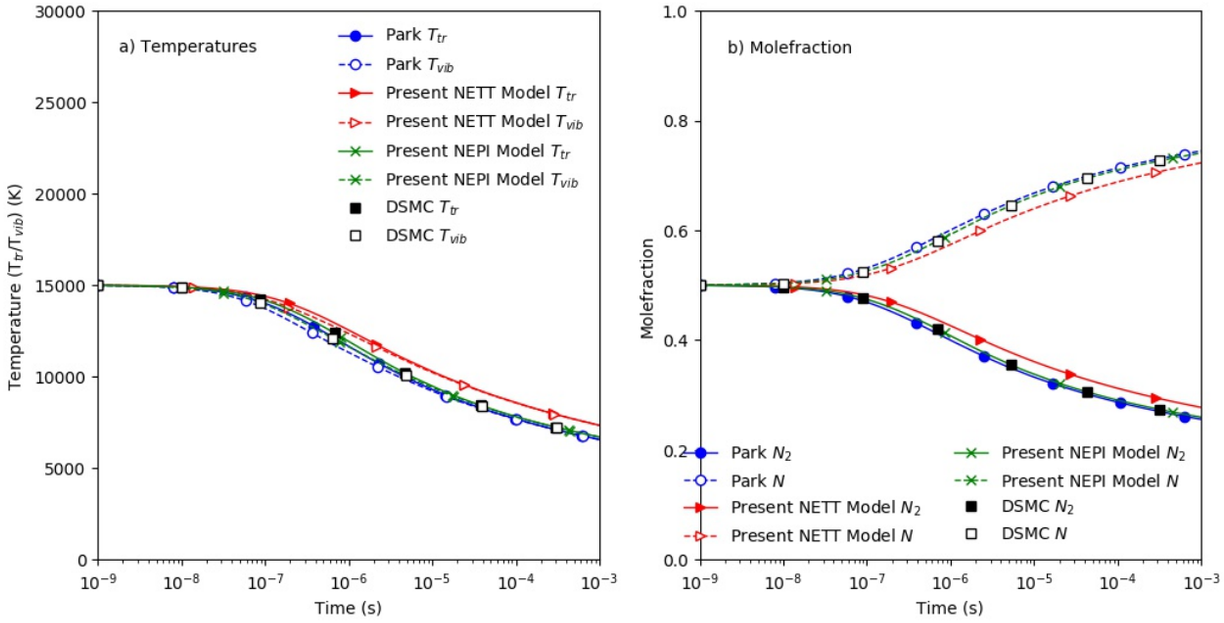

Fig. 5. Comparison of evolution of a) trans-rotational and vibrational temperatures b) mole fraction of N and N_2 for simulation starting with equilibrium conditions, $T_{tr} = T_{vib} = 15000$ K and employing Park's two temperature model, NETT model and NEPI model in NSF framework and DSMC simulation.

Figure 4 shows the evolution of trans-rotational and vibrational temperatures and the mole-fraction of atomic and molecular oxygen for simulations initialized at equilibrium conditions. It is apparent that, at equilibrium, the evolution of the system predicted by the three NSF chemical reaction models are in close agreement with each other. The minor difference between the properties calculated using the new non-equilibrium NEPI model and those predicted by Park's $\sqrt{TT_V}$ model is because of the gap between the equilibrium reaction rates for the dissociation $O_2 + O_2 \rightarrow O_2 + 2O$, as shown in Fig. 1 (b).

The equilibrium reaction rate coefficients predicted by the QCT cross-section database at high temperatures are higher than those predicted by Park's parameter for the Arrhenius fit. Higher reaction rate coefficients result in a higher degree of dissociation of the molecular oxygen in simulations with the new non-equilibrium models, compared to those in simulations with Park's model, as is apparent from Fig. 4 (b). The higher dissociation results are accompanied by higher energy expense needed for bond breaking, leading to lower temperatures.

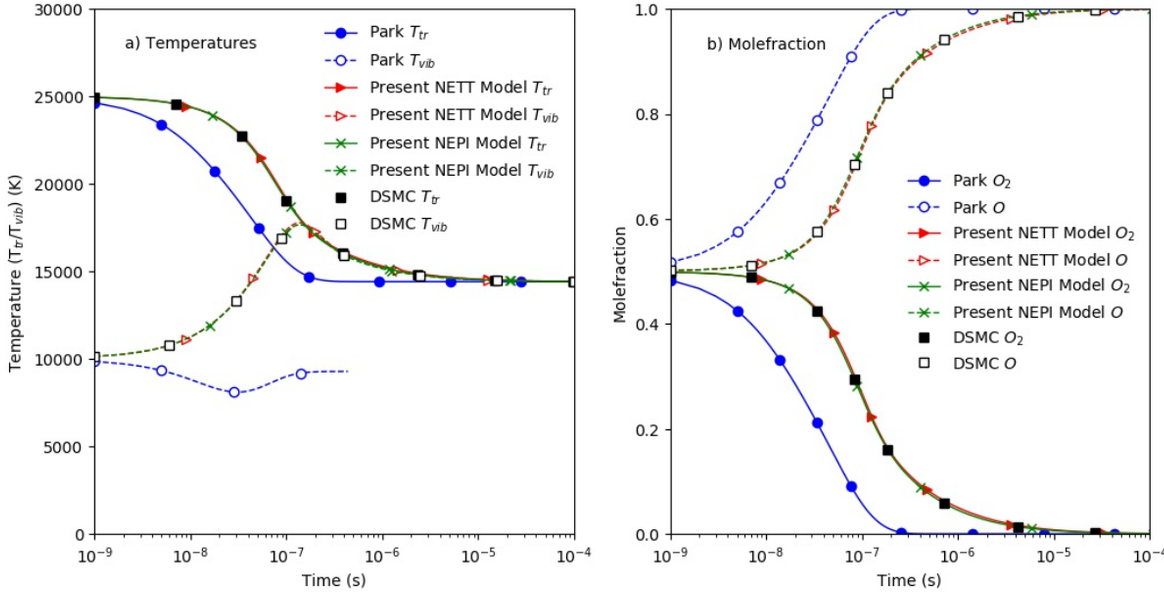

Fig. 6. Comparison of evolution of a) trans-rotational and vibrational temperatures b) mole fraction of O and O_2 for simulation starting with vibrationally cold conditions, T_{tr} =25000, T_{vib} =10000 K and employing Park's two temperature model, NETT model and NEPI model in NSF framework and DSMC simulation.

Figure 5 shows the evolution of properties for nitrogen systems. Like the observations made for oxygen systems, the degree of difference between the mole-fractions of the constituents and the temperatures predicted by the new non-equilibrium NEPI model and Park's two temperature

model is minor, again attributed to the gap in the equilibrium reaction rate coefficients predicted by the QCT based cross-sections and the Arrhenius fit proposed by Park. Although not shown in the figure, the performance of Park's two temperature with QK fitting parameters was found to be slightly better than Park's two temperature model with Park's original fitting parameters.

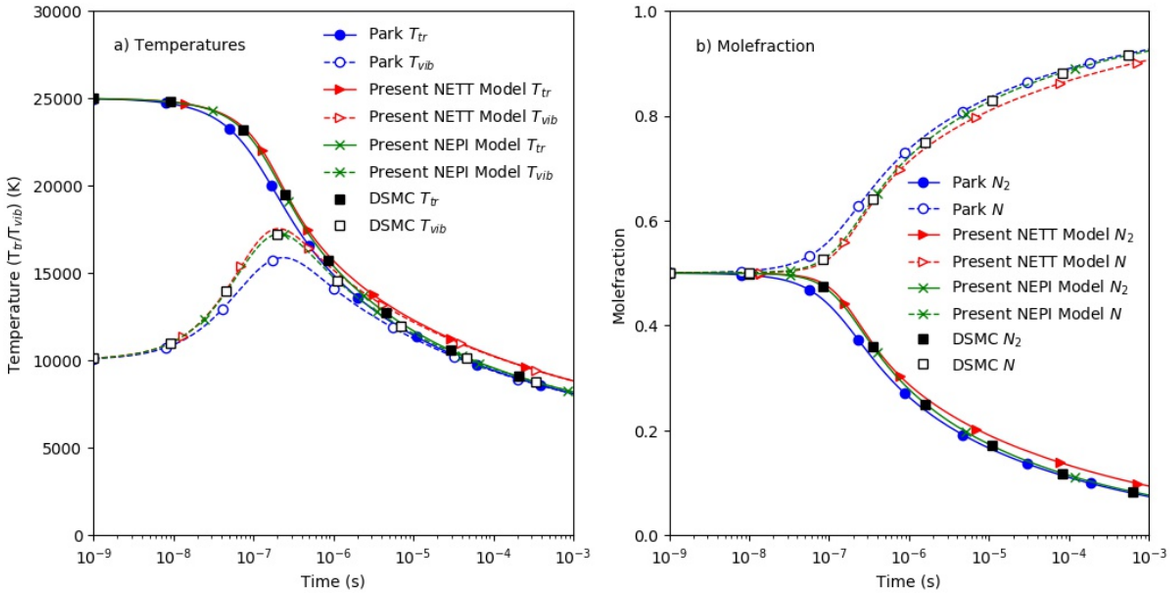

Fig. 7. Comparison of evolution of a) trans-rotational and vibrational temperatures b) mole fraction of N and N_2 for simulation starting with vibrationally cold conditions, T_{tr} =25000 K, T_{vib} =10000K and employing Park's two temperature model, NETT model and NEPI model in NSF framework and DSMC simulation.

For vibrationally cold initial conditions, however, the effect of non-equilibrium on the reaction rate coefficients, and further, on the temperatures and mole-fractions, is more distinct, as depicted in Figs. 6 and 7. Vibrationally cold simulations have a practical relevance because of theirs similarity to the flow in the shock region in hypersonic flows. It is known that the vibrational energy exchange has a longer relaxation time than the rotational and the translational

energy modes, which results in a vibrational temperature lower than the translational and the rotational temperatures in the shock and the post-shock regions.

At vibrationally cold conditions, it was shown (Figs. 2 and 3) that non-equilibrium reaction rate coefficients were much lower compared to the reaction rate coefficients calculated using Park's two temperature model. This leads to an initially lower degree of dissociation in molecular oxygen and nitrogen for simulations employing the new NETT and NEPI models, versus Park's two temperature model. As a result, the translational-vibrational energy exchange dominates over the dissociation mechanism leading to higher vibrational temperatures for the non-equilibrium models. For the nitrogen systems, the peak vibrational temperatures predicted by the NETT model, NEPI model, and Park's two temperature model were 17537, 17235 K and 15877 K, respectively. The analytical form of the NETT model was selected to accurately capture reaction rate coefficients in vibrationally cold non-equilibrium conditions. This leads to excellent agreement between the NETT and NEPI model for simulations with vibrationally cold and near equilibrium conditions. The peak vibrational temperature predicted by the NETT and NEPI models in oxygen system simulations were 17657 K and 17769 K, respectively. Again, the difference in temperatures and mole-fractions predicted by the new non-equilibrium models was negligible.

For the simulation with Park's two temperature model for the oxygen system, the high reaction rate coefficients caused a quick and full dissociation of molecular oxygen, especially from the higher vibrational levels, leading to a drastic decrease in vibrational temperature, as shown in Fig. 6 (a). Both systems proceed towards equilibrium conditions as time progresses and the degree of non-equilibrium is reduced. This leads to a better match between the new non-equilibrium models and Park's two temperature model. The progression of temperatures and

mole-fractions predicted by the DSMC simulation with the ab-initio based chemical reaction model matches well with those predicted by the new non-equilibrium models in the NSF framework. At the stated initial temperature conditions, the molecular oxygen fully dissociates to atomic oxygen, as is apparent from Fig. 6. Nitrogen starts to dissociate at a higher temperature compared to oxygen. In addition, the reaction rates for nitrogen dissociation are lower compared to those of oxygen systems, which leads to a lower degree of dissociation for nitrogen system.

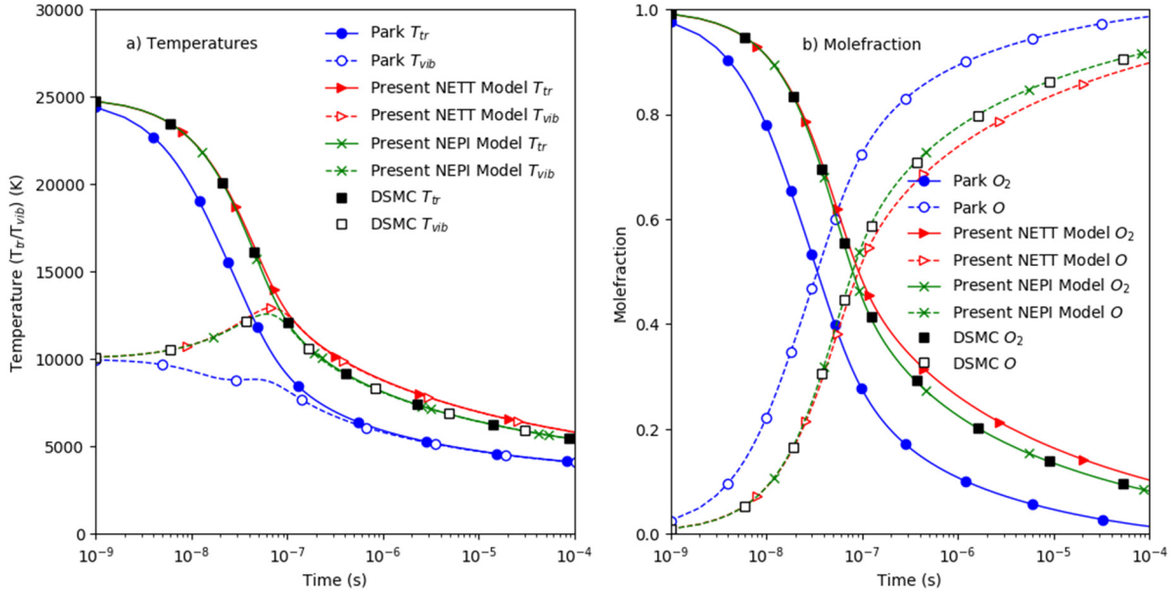

Fig. 8. Comparison of evolution of a) trans-rotational and vibrational temperatures b) mole fraction of O and O_2 for simulation starting with vibrationally cold conditions, T_{tr} =25000, T_{vib} =10000 K, initial O_2 mole fraction = 1, and employing Park's two temperature model, NETT model and NEPI model in NSF framework and DSMC simulation

The freestream conditions in case of realistic hypersonic flows comprise of gas in fully recombined molecular entities. Also, the conditions in the shock and post-shock regions are similar to those undertaken in the heat bath simulations at vibrationally cold initial conditions

presented here. Additional set of simulations for both oxygen and nitrogen is carried out with initial composition entirely made of molecules. The time evolution of various temperatures and mole-fraction of molecular and atomic entities on oxygen and nitrogen systems is shown in Figs. 8 and 9, respectively. Again, observations from this extra set of simulation are similar to those seen in the simulations shown in Figs. 6 and 7.

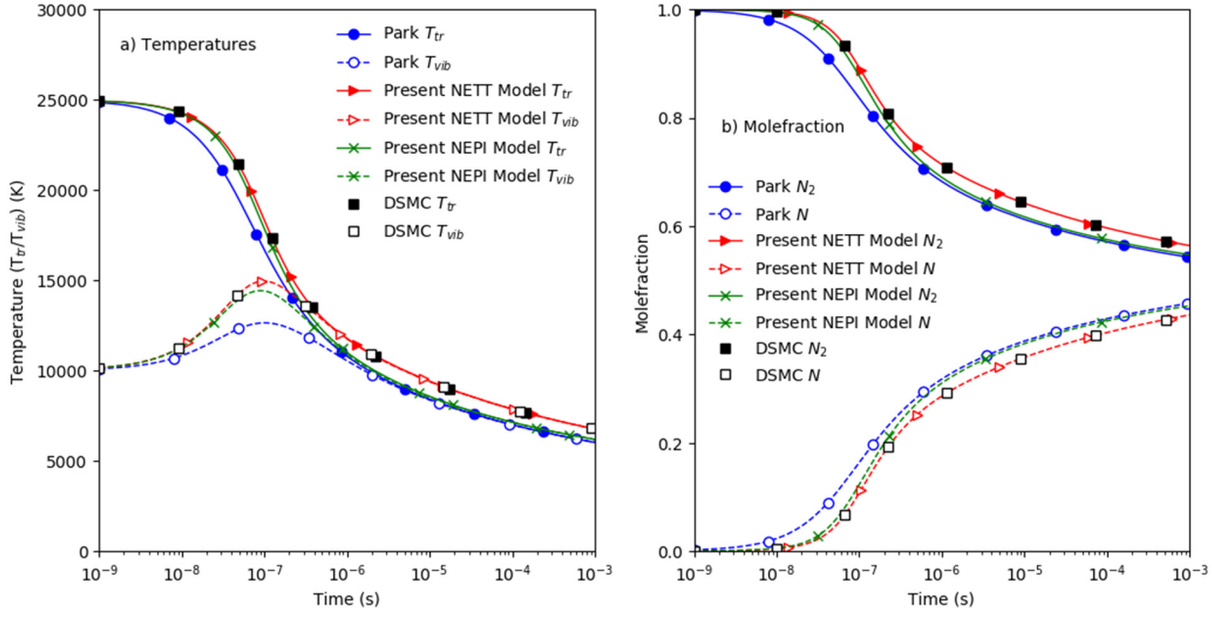

Fig. 9. Comparison of evolution of a) trans-rotational and vibrational temperatures b) mole fraction of N and N_2 for simulation starting with vibrationally cold conditions, T_{tr} =25000, T_{vib} =10000 K, initial N_2 mole fraction = 1, and employing Park's two temperature model, NETT model and NEPI model in NSF framework and DSMC simulation

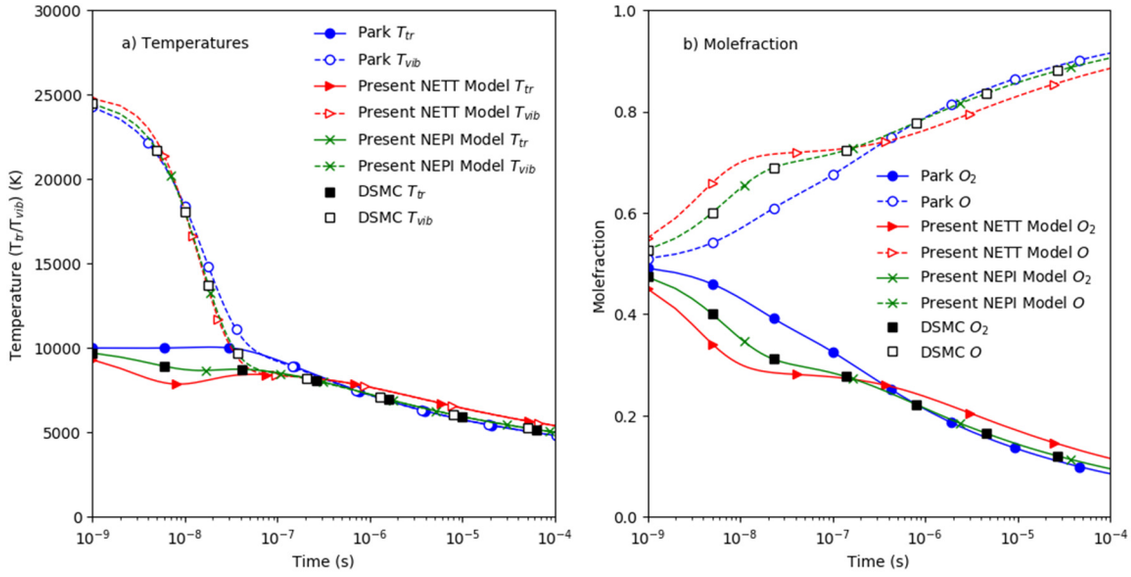

Fig. 10. Comparison of evolution of a) trans-rotational and vibrational temperatures b) mole fraction of O and O_2 for simulation starting with vibrationally hot conditions, T_{tr} =10000 K, T_{vib} =25000 K and employing Park's two temperature model, NETT model and NEPI model in NSF framework and DSMC simulation.

One of the possible scenarios where vibrationally hot conditions are expected to affect the flow chemistry occurs with expansion flow over a convex corner, resulting in a Prandtl-Meyer expansion fan. The vibrational temperature across the expansion fan relaxes at a slower rate than the translational temperature. The non-equilibrium conditions affect the forward reaction rate coefficients. The conventional way of handling the recombination is to employ an equilibrium constant and forward reaction rate coefficients. In this manner, the non-equilibrium conditions will also affect the recombination reaction rate coefficients.

Unlike the vibrationally cold conditions, the opposite results were obtained for heat bath simulations initialized at vibrationally hot conditions. Figures 10 and 11 show a) the relaxation of temperatures from vibrationally hot non-equilibrium conditions to the final single equilibrium

temperature, and b) the change in the constituting mole-fractions of the atomic and molecular entities with respect to time. The difference in the temperatures and the mole-fraction predicted by using the three chemical reaction models for either system is distinct and striking. Park's two temperature model under-predicts reaction rates compared to the QCT based non-equilibrium rates at vibrationally hot conditions, as noted in Figs. 2 and 3. As a result, the degree of dissociation in the simulation with Park's two temperature model is lower than those predicted by the new non-equilibrium models.

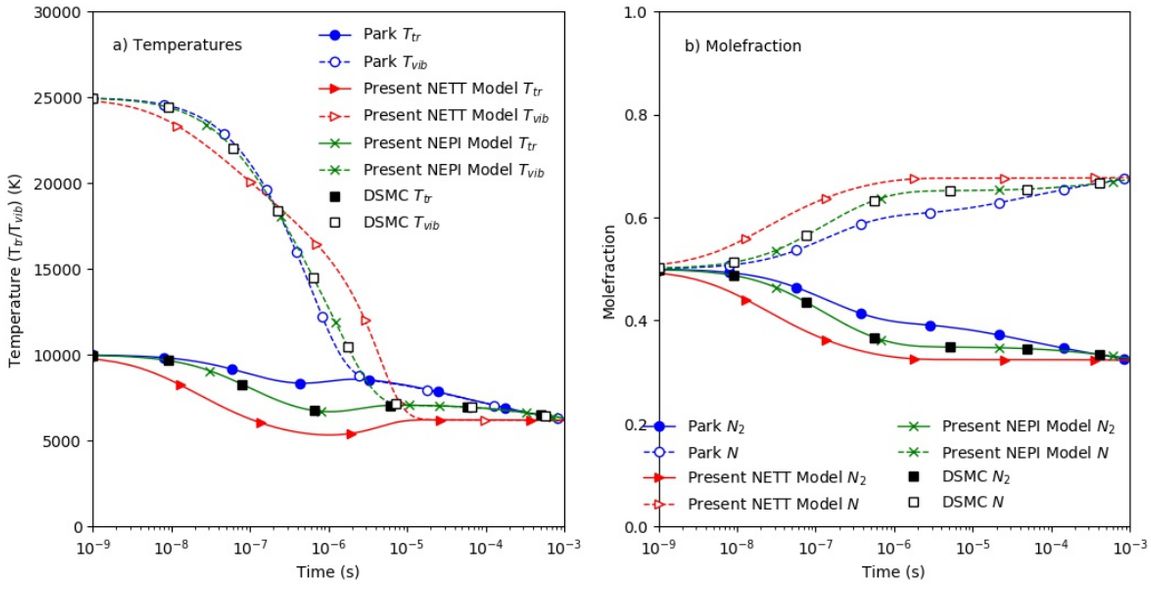

Fig. 11. Comparison of evolution of a) trans-rotational and vibrational temperatures b) mole fraction of N and N_2 for simulation starting with vibrationally hot conditions, T_{tr} =10000 K, T_{vib} =25000 K and employing Park's two temperature model, NETT model and NEPI model in NSF framework and DSMC simulation.

Moreover, the NETT model over-predicts the reaction rate coefficients compared to the NEPI model. This is a short-coming of the NETT model over the NEPI model. It is also apparent that the NEPI model matches well with the DSMC simulations employing the ab-initio based

chemical reaction model. For this reason, the NEPI model may be preferred over the NETT model for investigating scenarios at vibrationally hot conditions.

B. Shock Tube Simulation

Ibraguimova *et al*. [46] reported the vibrational temperature behind the shock front in a detonation shock tube at different temperature and pressure conditions. The driver side consisted of a mixture of hydrogen and oxygen diluted by helium, which was detonated using an electric pulse. The driver side consisted of pure molecular oxygen at 295 K. The two sides were separated by a copper diaphragm that ruptured after the electric pulse initiated combustion. The conditions of the shock tube were set in such a manner that the shock front traveled in the driven side at a velocity ranging between 3.07 - 4.44 km/s. The shock wave results in the dissociation of molecular oxygen and vibrational energy relaxation. The radiation probes in the test section measured the absorbance of oxygen molecules in the Schumann-Runge system, which is used to calculate the vibrational temperature. Several authors [28, 29, 47–49] have used the results of this experiment to investigate and validate non-equilibrium chemical reaction and chemistry-vibrational relaxation models.

The exact composition of the gas in the driver section at the time the diaphragm ruptures is not known. The pressure and temperature conditions on the driver sides were also not reported for the experiment. Designing a simulation that will reproduce the exact experiment is non-trivial at best. Various authors have employed different procedures to represent a computational equivalent of the experiment. Kim *et al*. [49] implemented a quasi-one dimensional shock tube code to validate their chemical reaction models with Ibraguimova *et al*.'s shock tube experiment. The validation of the 2-T chemical reaction model proposed by Kim *et al*. [49] and by the state-to-state model (with QCT Varandas rates) by Nietzel *et al*. [47, 48] was remarkably close to the

actual experimental results. The advantages and disadvantages of the various simulation methodologies implemented in the continuum NSF framework and in the particle method (DSMC) were discussed at length in the report by Wysong *et al*. [50]. In the present work, Wysong's *et al*. solution strategy [50] of simulating a two-dimensional flow around a blunt body was considered instead of the unsteady shock tube problem.

The dimensions of the domain and the flat blunt-body were the same as those assumed by Wysong *et al.* [50]. This was to ensure that the Knudsen number of the flow was low. This, in turn, ensures that the temperature and mole-fraction profiles at the stagnation line are equivalent to those in the one-dimensional shock tube case. The inlet and ambient conditions were initialized at the given driven side of the shock tube. The freestream conditions consisted of pure molecular oxygen.

In the present work, two cases at extreme conditions out of a series of experiments conducted by Ibraguimova *et al.*, at Mach numbers 9.3 and 13.4, are carried out. The grid and time independence studies have been carried out to verify the veracity of the final results. In addition to this, the recombination reactions have been ignored as per recommendation from the previous work [50].

Simulations at the two initial shock tube conditions were carried out with three different chemical reaction models, Park's two temperature model, the NETT model, and the NEPI model. Again, the hypersonic OpenFOAM solver, hy2Foam, was used for the simulations.

Figures 12 and 13 show a comparison of vibrational and trans-rotational temperatures, respectively, along the stagnation line in the post region obtained using the NSF simulations, employing the three chemical reaction models along with the experimental data. Figure 12 (a) shows the variation for the lower Mach number case (M = 9.3), while Fig. 12 (b) depicts the

comparison for the higher Mach number (M = 13.4). The observations made in the shock tube simulations are similar to those in the heat bath simulations with initial vibrationally cold conditions.

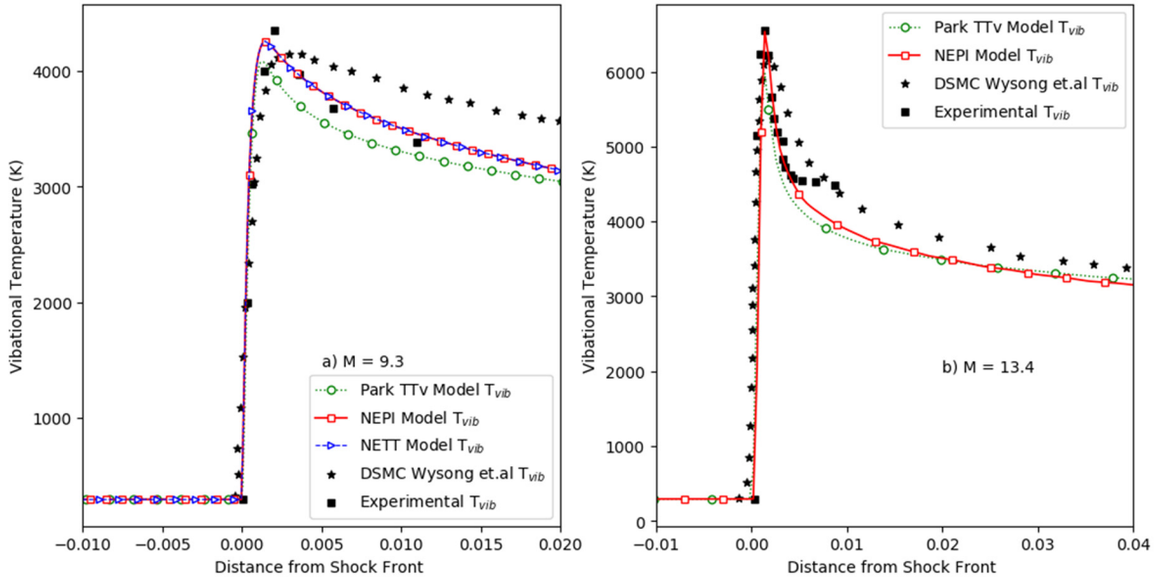

Fig. 12. Comparison of vibrational temperatures for shock tube simulation employing Park's two temperature model, NETT model and NEPI model in the NSF framework and the experimental results by Ibraguimova *et al*. [46], DSMC results by Wysong *et al*. [50].

The following observations are apparent from the vibrational temperature plots. Firstly, the results obtained from the simulations employing Park's two temperature model with parameters recommended by Park substantially disagree with the experimental data for both shock tube conditions. The experimental peak vibrational temperatures were 4352 K and 6548 K for Mach numbers 9.3 and 13.4, respectively. The peak temperature predicted by Park's two temperature model, the NETT model, and the NEPI model were 4079 K, 4260 K, and 4255 K, respectively, for M = 9.3, and 5976 K, 6861 K, and 6535 K, respectively, for M = 13.4. The position and the

value of the highest vibrational temperature along the stagnation line for simulations with Park's two temperature model are closer to the shock front and lower than the peak obtained in the experiments.

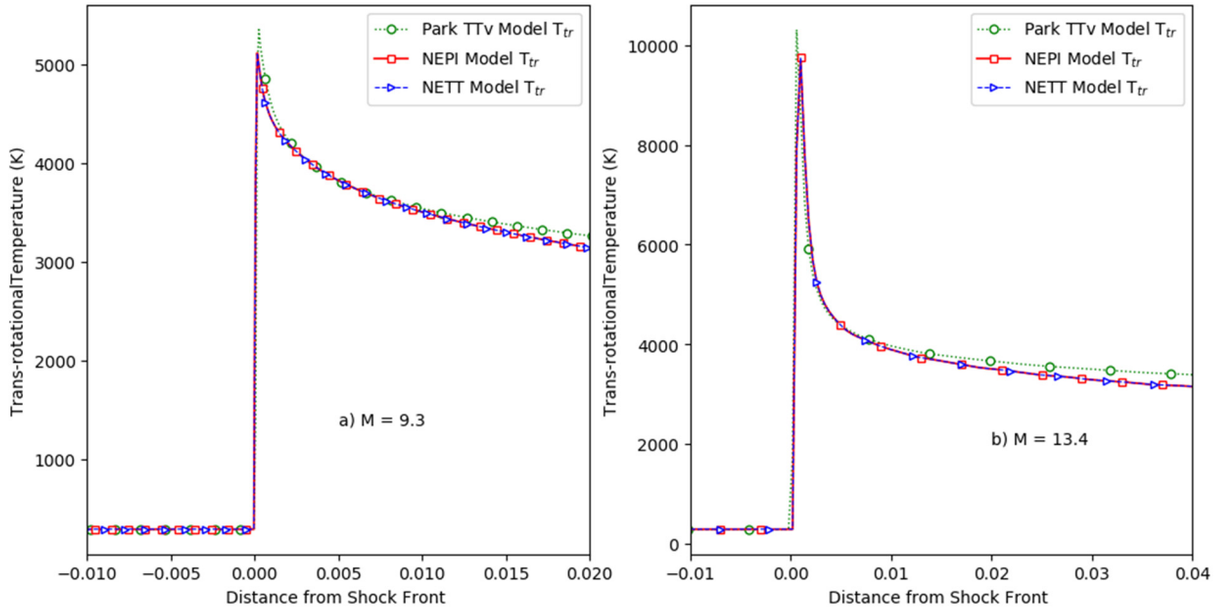

Fig. 13. Comparison of trans-rotational temperatures for shock tube simulation employing Park's two temperature model, NETT model and NEPI model in the NSF framework.

In comparison to this, the predictions by the new non-equilibrium models are in much better agreement with the experimental data. In particular, the NEPI model is in excellent agreement with the peak experimental vibrational temperature data. Additionally, the NETT model has a negligible discrepancy in the peak vibrational temperature at the higher Mach number shock tube simulations. A similar variation was observed in the vibrational temperatures predicted between the two new non-equilibrium models in the heat bath simulations with vibrationally cold initial conditions, as shown in Figs. 6 and 7 in the previous section. The difference between the two new non-equilibrium models for the remaining points on the stagnation line was found to be negligible.

The lower vibrational temperature is a direct consequence of the higher reaction rate coefficients predicted by Park's phenomenological model compared to the non-equilibrium reaction rate coefficients calculated using the QCT cross-sections database. It is also apparent from Fig. 12 (b), that the difference between the profiles predicted by the new non-equilibrium models (and the Park's two temperature model) and the experimental data is significant at points farthest from the shock front. Wysong *et al*. have also reported similar variations for the two-dimensional DSMC simulations. The focus in the present work is on calculating the non-equilibrium reaction rate coefficients, not on the translational-vibrational relaxation. This may be the reason for the gap in the computational results and the experimental data.

V. Conclusions and Remarks

The present work presents two new non-equilibrium reaction models, NETT and NEPI, for the continuum framework, by focusing on matching the reaction rate coefficients calculated using the QCT based dissociation cross-section database. Heat bath simulations showed that the new non-equilibrium models, NETT and NEPI, were superior to traditional phenomenological models such as Park's two temperature model, especially for equilibrium and vibrationally cold conditions. For the vibrationally hot non-equilibrium, where the vibrational temperature is greater than the trans-rotational temperature, the NEPI model predicted various modes of temperatures and mole-fractions of constituent species which agreed remarkably well with the DSMC simulations using the ab-initio based chemical reaction model. In contrast, the NETT model over-predicted the reaction rate coefficients, and Park's two temperature model under-predicted the reaction rate coefficients for vibrationally hot conditions.

The models were further tested for shock tube simulations, focusing on validation and comparison with vibrational temperatures measured by experimental work. The two-dimensional

studies showed that the new non-equilibrium models were more accurate compared to the traditional approach and in closer agreement with the experimental data. They correctly predicted the position and the peak value of the vibrational temperature. Additionally, the new models had relatively minor computation overheads. The present work, consistent with state-specific ab-initio based chemical reaction models for non-equilibrium flows, provides the obvious benefits over phenomenological models.

In the shock-tube validation studies, the peak temperature in the shock front was captured well using the new chemical reaction models with NSF equations. However, the temperature profiles in the post-shock region obtained in the present work did not match well with those observed in the experiments at higher Mach number. As future work, these non-equilibrium chemical reaction models will be added to the NCCR framework in order to understand the interaction between the second-order thermal non-equilibrium effects and chemical non-equilibrium.

VI. Supplementary Materials

The fitting parameters for the NEPI model fitting scheme for all four dissociations and QCT generated non-equilibrium data as a function of trans-rotational and vibrational temperatures are tabulated in the supplementary material. Relevant C++ files for the NETT and NEPI implementations added to the existing database of chemical reaction models in hy2Foam solver are also provided with the supplementary materials.

VII. Acknowledgment

This work was supported by the National Research Foundation of Korea (NRF) Grant funded by the Ministry of Science, ICT & Future Planning (NRF 2017-R1A2B2007634 and 2017-M1A3A3A03016312) South Korea.

References

[1] G. V. Candler and I. Nompelis, "Computational fluid dynamics for atmospheric entry," Technical Report (Minnesota Univ. Minneapolis Dept. of Aerospace Engineering and Mechanics, 2009).

[2] C. Park*, Nonequilibrium Hypersonic Aerothermodynamics* (Wiley, New York, 1990).

[3] G. A. Bird, "Direct simulation and the Boltzmann equation," Physics of Fluids, **13**, 2676 (1970).

[4] G. A. Bird, M. Gallis, J. Torczynski, and D. Rader, "Accuracy and efficiency of the sophisticated direct simulation Monte Carlo algorithm for simulating non-continuum gas flows," Physics of Fluids, **21**, 017103 (2009).

[5] S. K. Stefanov, "On the basic concepts of the direct simulation Monte Carlo method," Physics of Fluids, **31**, 067104 (2019).

[6] R. S. Myong, A. Karchani, and O. Ejtehadi, "A review and perspective on a convergence analysis of the direct simulation Monte Carlo and solution verification," Physics of Fluids, **31**, 066101, (2019).

[7] C. Borgnakke and P. S. Larsen, "Statistical collision model for Monte Carlo simulation of polyatomic gas mixture," Journal of Computational Physics, 18, 405 (1975).

[8] G. Bird, "Simulation of multi-dimensional and chemically reacting flows (past space shuttle orbiter)," Proceedings of International Symposium on Rarefied Gas Dynamics, 365-388, (1979).

[9] G. A. Bird, "The QK model for gas phase chemical reaction rates," Physics of Fluids, **23**, 106101 (2011).

[10] S. F. Gimelshein and I. J. Wysong, "Bird's total collision energy model: 4 decades and going strong," Physics of Fluids, **31**, 076101, (2019).

[11] D. G. Truhlar and J. T. Muckerman, *Reactive Scattering Cross Sections III: Quasiclassical and Semiclassical Methods* (Springer US, 1979).

[12] C. E. Treanor and P. V. Marrone, "Effect of dissociation on the rate of vibrational relaxation," The Physics of Fluids, **5**, 1022 (1962).

[13] S. O. Macheret and J. W. Rich, "Nonequilibrium dissociation rates behind strong shock waves: classical model," Chemical Physics, **174**, 25 (1993).

[14] M. Panesi, R. L. Jaffe, D. W. Schwenke, and T. E. Magin, "Rovibrational internal energy transfer and dissociation of $N_2(^1\sigma_{g+})$ - $N(^4S_u)$ system in hypersonic flows," The Journal of Chemical Physics, **138**, 044312, (2013).

[15] J. D. Bender, I. Nompelis, P. Valentini, S. Doraiswamy, T. E. Schwartzentruber, G. V. Candler, Y. Paukku, K. R. Yang, Z. Varga, and D. G. Truhlar, "Quasiclassical trajectory analysis of the N2 + N2 reaction using a new ab initio potential energy surface," in 11th AIAA/ASME Joint Thermophysics and Heat Transfer Conference, p. 2964 (Atlanta, USA, 2014).

[16] S. Voelkel, P. L. Varghese, and V. Raman, "Multi-temperature dissociation rate of N2+N2 → N2+N+N calculated using selective sampling quasi-classical trajectory analysis," Journal of Thermophysics and Heat Transfer, **31**, 965 (2017).

[17] I. Borges Sebastião, M. Kulakhmetov, and A. Alexeenko, "DSMC study of oxygen shock waves based on high-fidelity vibrational relaxation and dissociation models," Physics of Fluids, **29**, 017102 (2017).

[18] R. S. Chaudhry, M. S. Grover, J. D. Bender, T. E. Schwartzentruber, and G. V. Candler, " Quasiclassical trajectory analysis of oxygen dissociation via O2, O, and N2," AIAA Aerospace Sciences Meeting, Paper 0237 (2018).

[19] N. Singh and T. Schwartzentruber, "Nonequilibrium internal energy distributions during dissociation," Proceedings of the National Academy of Sciences, **115**, 47 (2018).

[20] R. S. Chaudhry, N. Singh, M. S. Grover, T. E. Schwartzentruber, and G. V. Candler, "Implementation of a nitrogen chemical kinetics model based on ab-initio data for hypersonic CFD," Joint Thermophysics and Heat Transfer Conference, Paper 3439 (2018).

[21] T. E. Magin, M. Panesi, A. Bourdon, R. L. Jaffe, and D. W. Schwenke, "Coarse-grain model for internal energy excitation and dissociation of molecular nitrogen," Chemical Physics, **398**, 90 (2012).

[22] A. Munafo, M. Panesi, and T. Magin, "Boltzmann rovibrational collisional coarse-grained model for internal energy excitation and dissociation in hypersonic flows," Physical Review E, **89**, 023001 (2014).

[23] A. Munafo, Y. Liu, and M. Panesi, "Modeling of dissociation and energy transfer in shock heated nitrogen flows," Physics of Fluids, **27**, 127101 (2015).

[24] R. Macdonald, R. Jaffe, D. Schwenke, and M. Panesi, "Construction of a coarse-grain quasi classical trajectory method: I. Theory and application to N2-N2 system," The Journal of Chemical Physics, **148**, 054309 (2018).

[25] R. Macdonald, M. Grover, T. E. Schwartzentruber, and M. Panesi, "Construction of a coarse-grain quasi-classical trajectory method: II. Comparison against the direct molecular simulation method," The Journal of Chemical Physics, **148**, 054310 (2018).

[26] H. Luo, M. Kulakhmetov, and A. Alexeenko, "Ab initio state-specific N2+O dissociation and exchange modeling for molecular simulations," The Journal of Chemical Physics, **146**, 074303 (2017).

[27] H. Luo, A. A. Alexeenko, and S. O. Macheret, "Development of an impulsive model of dissociation in direct simulation Monte Carlo," Physics of Fluids, **31**, 087105 (2019).

[28] D. A. Andrienko and I. D. Boyd, "State-specific dissociation in O2-O2 collisions by quasi-classical trajectory method," Chemical Physics, **491**, 74 (2017).

[29] J. Hao and C. Wen, "Stabilization of a Mach 6 boundary layer using a two-dimensional cavity," AIAA Scitech Forum, p. 1131 (San Diego, USA, 2019).

[30] T. K. Mankodi, U. V. Bhandarkar, and B. P. Puranik, "Dissociation cross sections for N2+N→3N and O2+O→3O using the QCT method," The Journal of Chemical Physics, **146**, 204307 (2017).

[31] T. K. Mankodi, U. V. Bhandarkar, and B. P. Puranik, "An ab initio chemical reaction model for the direct simulation Monte Carlo study of non-equilibrium nitrogen flows," The Journal of Chemical Physics, **147**, 084305 (2017).

[32] T. K. Mankodi, U. V. Bhandarkar, and B. P. Puranik, "Dissociation cross-sections for high energy O2-O2 collisions," The Journal of Chemical Physics, **148**, 144305 (2018).

[33] R. S. Myong, "Thermodynamically consistent hydrodynamic computational models for high Knudsen-number gas flows," Physics of Fluids, **11**, 2788 (1999).

[34] R. S. Myong, "On the high Mach number shock structure singularity caused by overreach of Maxwellian molecules," Physics of Fluids, **26**, 056102 (2014).

[35] Y. Paukku, K. R. Yang, Z. Varga, and D. G. Truhlar, "Global ab initio ground-state potential energy surface of N4," The Journal of Chemical Physics, **139**, 044309 (2013).

[36] Y. Paukku, Z. Varga, and D. G. Truhlar, "Potential energy surface of triplet O4," The Journal of Chemical Physics, **148**, 124314 (2018).

[37] R. J. Duchovic, Y. L. Volobuev, G. C. Lynch, D. G. Truhlar, T. C. Allison, A. F. Wagner, B. C. Garrett, and J. C. Corchado, "PotLIB 2001: A potential energy surface library for chemical systems," Computer Physics Communications, **2**, 169 (2002).

[38] S. R. Byron, "Measurement of the rate of dissociation of oxygen," The Journal of Chemical Physics, **30**, 1380 (1959).

[39] B. Cary, "Shock-tube study of the thermal dissociation of nitrogen," Physics of Fluids, **8**, 26 (1965).

[40] J. P. Appleton, M. Steinberg, and D. Liquornik, "Shock-tube study of nitrogen dissociation using vacuum-ultraviolet light absorption," The Journal of Chemical Physics, **48**, 599 (1968).

[41] R. K. Hanson and D. Baganoff, "Shock-Tube Study of Nitrogen Dissociation Rates Using Pressure Measurements," AIAA Journal, **10**, 211 (1972).

[42] O. P. Shatalov, "Molecular dissociation of oxygen in the absence of vibrational equilibrium," Combustion, Explosion and Shock Waves, **9**, 610 (1973).

[43] D. Baulch, *Evaluated Kinetic Data for High Temperature Reactions. Homogeneous Gas Phase Reactions of the H2-N2-O2 System*, (Butterworths, 1973).

[44] T. J. Scanlon, C. White, M. K. Borg, R. C. Palharini, E. Farbar, I. D. Boyd, J. M. Reese, and R. E. Brown, "Open-source direct simulation Monte Carlo chemistry modeling for hypersonic flows," AIAA Journal, **53**, 1670 (2015).

[45] M. A. Gallis, R. B. Bond, and J. R. Torczynski, "A kinetic-theory approach for computing chemical-reaction rates in upper-atmosphere hypersonic flows," The Journal of Chemical Physics, **131**, 124311 (2009).

[46] L. Ibraguimova, A. Sergievskaya, V. Y. Levashov, O. Shatalov, Y. V. Tunik, and I. Zabelinskii, "Investigation of oxygen dissociation and vibrational relaxation at temperatures 4000-10800k," The Journal of Chemical Physics, **139**, 034317 (2013).

[47] K. Neitzel, D. Andrienko, and I. D. Boyd, "Modeling fidelity for oxygen nonequilibrium thermochemistry in reflected shock tube flows", in 45th AIAA Thermophysics Conference, p. 2509 (Dallas, USA, 2015).

[48] K. Neitzel, D. Andrienko, and I. D. Boyd, "Thermochemical nonequilibrium modeling for hypersonic flows containing oxygen", in 46th AIAA Thermophysics Conference, p. 4023 (Washington, USA, 2015).

[49] J. G. Kim and G. Park, "Thermochemical non-equilibrium parameter modification of oxygen for a two-temperature model," Physics of Fluids, **30**, 016101 (2018).

[50] I. Wysong, S. Gimelshein, Y. Bondar, and M. Ivanov, "Comparison of direct simulation Monte Carlo chemistry and vibrational models applied to oxygen shock measurements," Physics of Fluids, **26**, 043101 (2014).